Materials Physics and Mechanics 14 (2012) 129-136 Received: June 1, 2012

COMPARATIVE STUDY OF STRUCTURAL, MORPHOLOGICAL AND OPTICAL CHARACTERIZATION OF CdS, CdAlS AND CdAlS ANNEALED THIN FILMS

L.S. Ravangave[1*], S.D. Misal[2], U.V. Biradar[3], K.N. Rothod[4]

[1] Department of Physics, Shri Sant Gadge Maharaj College, Loha (M.S.), India.

[2]Department of Physics, Kumar Swami College, Ausa (M.S.), India.

[3]Department of Physics, Mahatma Basweshwar College, Latur (M.S.), India.

[4]Department of Physics, Dayanand Science College, Latur (M.S.), India.

*e-mail: lsravangave@gmail.com

Abstract. Chemical Bath Deposition (CBD) technique was used for preparation of CdS, and Al doped CdS thin films. Al doped CdS films were annealed at different temperatures in air. CdS, as- deposited Al doped CdS and annealed Al doped CdS films were characterized using XRD, Scanning Electron Microscopy (SEM) and UV-Visible spectrophotometer. XRD study revealed the hexagonal phase of CdS and Al doped CdS material in the thin films. The XRD study shows that the hexagonal structure of CdS is not much affected with respect to Al doping. Al doped films annealed above 473 K crystalline phase of CdS transform into polycrystalline. The variations of lattice parameters and grain size with annealing temperature were investigated from XRD data. The % transmittance and optical band gap were investigated from optical data. The optical band gap of Al doped CdS films annealed at 473 K and 573 K is increased as compare to CdS (2.42 eV).

1. Introduction

The II-VI compound semiconductors are of great importance due to their applications in various electro-optic devices. Cadmium sulphide (CdS) is a wide band gap semiconductor belonging to II-VI group compounds [1-3]. CBD is a low-cost, relatively simple and practical method for covering complex substrates [4], and offers excellent control when depositing thinner films. For the application of CdS thin films in solar cells, it is necessary to have layers with the following characteristics: i) uniformity, ii) transparency, iii) crystallinity, and iv) good electrical properties. Cadmium sulfide (CdS) is a wide band gap (2.42 eV) and direct transition semiconductor [5].

Consequently, it is potentially an important material to be used as an antireflection coating for heterojunction solar cells [6]. It has been widely used as a window material in high efficiency thin film solar cells based on CdTe or CIGS [7].

The addition of trace amount of transition metal ion into CdS host plays an important role in modifying the structural, optical and electrical transport properties of the binary alloy material [8]. Metal chalcogenides are attracting a great deal of attention because of their many fold importance in a wide spectrum of optoelectronics devices [9].

Al-doped CdS thin films show low electrical resistivity of about 48 Ω cm and high carrier density of about 1.1×1019 cm^{-3}. The doping of group III elements has been found to decrease the resistivity of CdS thin films. The effect of Al incorporation on the structural and

hexagonal planes of the CdS and Al doped CdS thin films were calculated from XRD data using the following equation

$$\cdot \frac{1}{d^2} = \frac{4}{3}\frac{(h^2 + hk + k^2)}{a^2} + \frac{l^2}{c^2} \cdot \quad (1)$$

The calculated values of lattice constant *a* and *c* are 4.118 nm (4.121 nm) and 6.759 nm (6.682 nm) respectively. The quantities in the parentheses shows the values of ***a*** and *c* obtained from standard JCPDS card 80-0006. The calculated values of *a* and *c* are very close to observed values of CdS thin films. The values of lattice constants *a* and *c* are observed decreased on doping of Al. The effect of annealing temperature was clearly observed on lattice constants; the variation was displayed in Table 1 and presented in Fig. 2.

The grain size was calculated from XRD data using Sherrie's formula [12]:

$$D = \frac{0.94\lambda}{\beta \cos\theta}, \quad (2)$$

where λ is the wave length of X-ray used (1.54 nm $Cuk_{\alpha\ line}$), β is the broadening of the diffraction peak measured at half of its maximum intensity (FWHM) and θ is the Braggs angle. Table 1 shows the variation of grain size with Al doping and annealing temperature, and presented in Fig 3. The grain size of the CdS was observed increased on Al doping. Further the grain size is decreased for annealed films as compared to as-deposited Al doped CdS films. The average grain size of pure CdS thin film is 3.5 nm and 26 nm for Al doped CdS films.

Table 1. Variations of lattice constants, grain size and optical band with temperature.

Film type	Annealing Temp., K	Lattice constants '*a*', nm	Lattice constants '*c*', nm	Grain size, nm	Thickness, μm	Band Gap E_g, eV
CdS 300 K	300	4.1018	6.759	3.5	1.52	2.421
CdAlS as-deposited K	300	4.0431	6.486	26	1.22	2.29
Annealed at 373 K	373	4.277	6.5	20	0.87	2.31
Annealed at 473 K	473	4.041	6.486	8	1.21	2.70
Annealed at 573 K	573	4.444	6.584	10	1.23	2. 82

SEM (Scanning Electron Microscopy) images are displayed in Fig. 4 for pure CdS, as-deposited Al doped CdS and Al doped CdS films annealed at 473 K. SEM image for purely CdS film compactness was high, the surface's uniformity was good, the particle size was quite fine, and the particle size distribution was also narrow. These characteristics are in good agreement with the film's high transparency. Some of the larger sized grains assigned to colloidal particles of S ions. Al doping did not have significant effect on the surface morphology of CdS thin film. There are some spheroid shape growth appears as the creation of nucleation centre on the film surface. These shapes are more visible in Fig. 4 (2 -3). These are most probably aggregated due to colloidal particles formed in solution and then absorbed on the film.

The SEM image of Al doped CdS film annealed at 473 K shows increase in uniformity of the CdS film and smaller size Al granules are homogeneously substituted in the CdS phase of film. Over the highly compact Al doped CdS phase slightly higher density of scattered

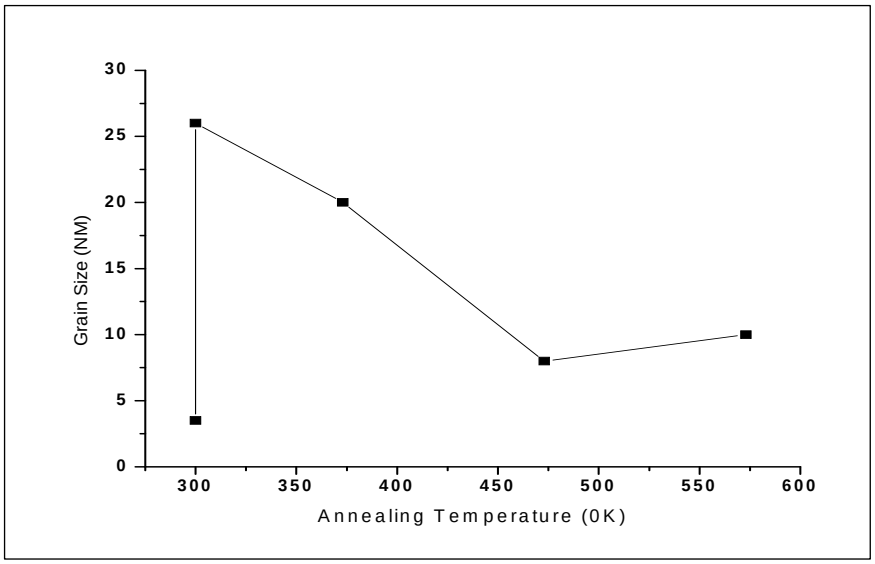

Fig. 3. Variation of grain size against annealed temperatures.

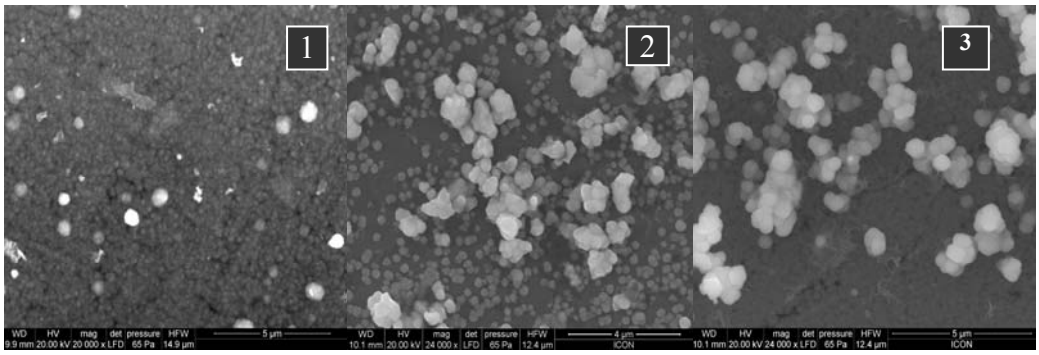

Fig. 4. SEM images for 1) pure CdS thin film, 2) as-deposited Al doped CdS thin film, and 3) annealed at 473 K.

Transmittance spectra are recorded in the wavelength range 350 to 800 nm using Systronics double beam 2201 spectrophotometer, and presented in Fig. 5 (1-5). The maximum transmittance was observed for all the films in the visible region. The maximum transmittance for pure CdS, as-deposited Al doped CdS, Al doped CdS annealed at 373 K and 473 K was observed 48.9 percent. For pure CdS thin film optical transmittance was 52 percent before the absorption edge. The % transmittance was observed decreased for Al doped CdS thin film and annealed Al doped CdS thin films. For Al doped CdS thin film annealed at 473 K the transmittance was observed increased as compared to as-deposited and annealed at 373 K and 573 K CdS thin films. The effect of Al doping and annealing also assigned to red shift of the absorption edge by approximately 50 nm as compared to pure CdS thin film.

The optical absorption of the pure CdS, as-deposited Al doped CdS films and Al doped CdS films annealed at different temperatures are presented in Fig. 6 (1-5). The spectra have been used to evaluate the absorption coefficient (α), energy band gap (E_g) and nature of transition involved. Optical energy band gap (E_g) can be calculated using [12]:

$$\alpha = \frac{A}{h\nu}(h\nu - E_g)^{1/2}. \tag{3}$$

Here A is the constant, $h\nu$ is the photon energy.

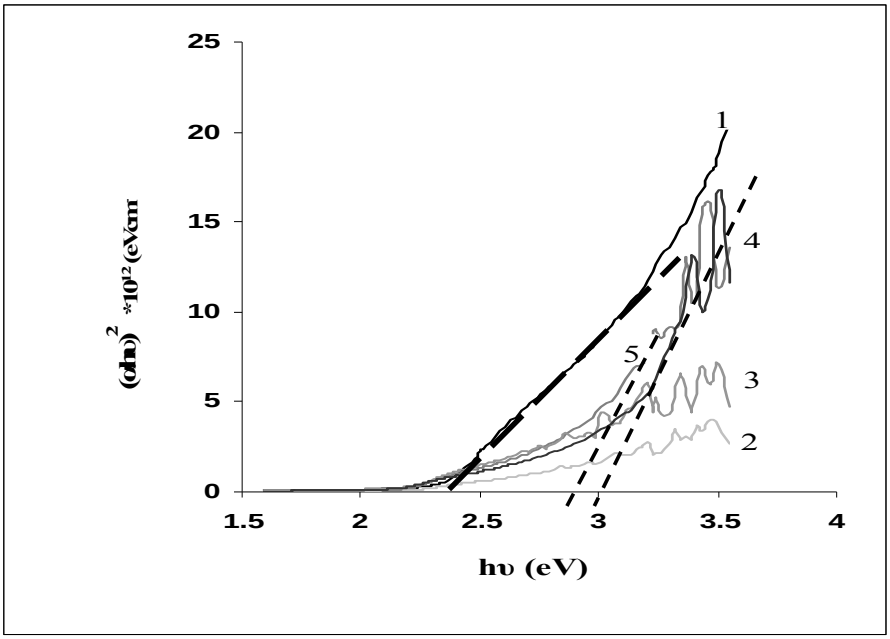

Fig. 7. Plot of $(\alpha h\nu)^2$ against $h\nu$ for 1) pure CdS, 2) As-deposited Al doped CdS films 3) annealed Al doped CdS film at 373 K, 4) annealed at 473 K, 5) annealed at 573 K.

The spectra shows that the absorption edges are red shifted. The experimental values of $(\alpha h\nu)^2$ obtained from absorption data and plotted against $h\nu$ for all films was shown in Fig. 7 (1-5). All the films show high absorption coefficient ($\alpha = 10^{12}$ cm^{-1}). The linear portion of the curve extrapolated to $(\alpha h\nu)^2 = 0$ gives the value of optical energy band gap (E_g). The optical band gap E_g obtained at $(\alpha h\nu)^2 = 0$ was vary from 2.29 to 2.81 eV and attains maximum of 2.71 eV and 2.81 eV for Al doped CDS film annealed at 473 K and 573 K respectively. The value of E_g for purely CdS film was observed 2.4211 eV which represent the standard value of (direct band gap semiconductor) CdS. The variation of optical band gap with annealing temperature is shown in Table 1. It was observed that optical band gap decreased for as-deposited Al doped CdS film as compared to purely CdS film. The effect of annealing leads to increase the band gap of Al doped film as compared to purely CdS annealed at 473 K and 573 K.

4. Conclusion

CdS and Al doped CdS thin Films were successfully synthesized using aqueous solutions of $CdCl_2$, $(Al)_2(SO_4)_3$ and $(NH_2)_2CS$ using Chemical Bath Deposition technique. The XRD study revealed the hexagonal phase of the Purely CdS and Al doped CdS thin films. From XRD data it is concluded that Al doped CdS phase homogeneously substituted with CdS phase at 473 K annealing temperature. The XRD study shows that the hexagonal structure of CdS is not much affected with respect to Al doping. The grain size is observed increased with Al doping and decreased with annealing. The variation of lattice parameters was observed decreased with Al doping and annealing. SEM study confirms that Al doping did not have significant effect on the surface morphology of CdS thin film. The Al doped thin film annealed at 473 K shows increase in uniformity of the CdS film and smaller size Al granules are homogeneously substituted in the CdS phase of film. The % transmittance was observed maximum in the visible region. The transmittance and absorption spectra showed the red shift of the absorption edge. Optical study confirmed that energy band gap of CdS, (direct band gap semiconductor),

was 2.42 changes with Al doping and annealing. The maximum 2.71 and 2.81 eV band gap was observed for Al doped CdS film annealed at 473 K and 573 K respectively.

Acknowledgements
The author wish to thank U.G.C. India, for financial assistance under MRP-XI Plan.

References
[1] G.E. Delgado, J.E. Contreras, A.J. Mora, L. Béancourt, P. Grima-Gallardo, M. Quintero // *Chalcogenide Lett.* **6 (12)** (2009) 647.
[2] H. Chavez, M. Jorden, J.C. McClure, G. Lush, V.P. Singh // *J. Mat. Sci.: Mater. Electron.* **8** (1997) 151.
[3] C.S. Ferekides, D. Marinskiy, S. Marinskaya, B. Tetali, D. Oman, D.L. Morel, In: *Proceedings 25th IEEE PVSC* (Washington, D.C., 1996) *p.* 751.
[4] I. Kaur, D.K. Pandya, K.L. Chopra // *J. Electrochem. Soc*. **127** (1980) 943.
[5] D. Kaushik, R.R. Singh, M. Sharma, D.K. Gupta, N.P. Lalla, R.K. Pandey // *Thin Solid Films* **515** (2007) 7070.
[6] I.O. Oladeji, L. Chow, C. Ferekides, V. Viswanathan, Z. Zhao // *Energy Mater. Sol. Cells.* **61** (2000) 203.
[7] O. Vigil-Galan, J. Ximello-Quiebras, J. Aguilar-Hernandez, G. Contreras-Puenta, A. Cruz Orea, J. Mendoza-Alverez, J. Gardona-Bedoya, C. Ruiz, V. Bermudez // *Semicond. Sci. Technol.* **21** (2006) 76.
[8] A. Ashour, H.H. Afify, S.A. Mahmoud // *Thin Solid Films* **248** (1994)253.
[9] B. Thangaraju // *Thin Solid Films* **71** (2002) 402.
[10] B.N. Patil, D.B. Naik, V.S. Shrivastava // *Chalcogenide letters* **8(2)** (2011) 117.
[11] J. Santos Cruz, R. Castanedo Pérez, G. Torres Delgado, O. Zelaya Angel // *Thin Solid Films* **518** (2010) 1791.
[12] L.V. Azaroff, *Elements of X-ray Crystallography* (McGraw –Hill Company, New York, 1968).
[13] S.D. Chavhan, S. Senthilarasu, Lee Soo-Hyoung // *Applied Surface Science* **254** (2008) 4539.